pubs.acs.org/Biomac

Article

Environmentally Benign Fast-Degrading Conductive Composites

Angelique F. Greene,* Robert Abbel, Alankar A. Vaidya, Queenie Tanjay, Yi Chen, Regis Risani, Taryn Saggese, Maxime Barbier, Miruna Petcu, Mark West, Beatrix Theobald, Eva Gaugler, and Kate Parker

Cite This: *Biomacromolecules* 2024, 25, 455−465

Read Online

ACCESS | Metrics & More | Article Recommendations | Supporting Information

Downloaded via SCION RESEARCH on January 24, 2024 at 21:57:50 (UTC).
See https://pubs.acs.org/sharingguidelines for options on how to legitimately share published articles.

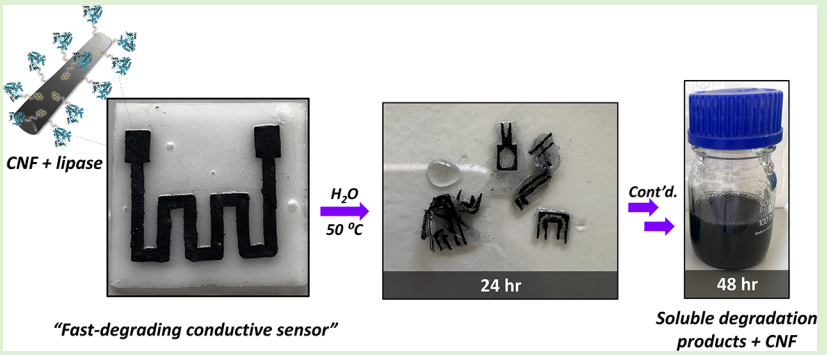

ABSTRACT: An environmentally benign conductive composite that rapidly degrades in the presence of warm water via enzyme-mediated hydrolysis is described. This represents the first time that hydrolytic enzymes have been immobilized onto eco-friendly conductive carbon sources with the express purpose of degrading the encapsulating biodegradable plastic. Amano Lipase (AL)-functionalized carbon nanofibers (CNF) were compounded with polycaprolactone (PCL) to produce the composite film CNF_{AL}-PCL (thickness ∼ 600 μm; CNF_{AL} = 20.0 wt %). To serve as controls, films of the same thickness were also produced, including CNF-AL_5-PCL (CNF mixed with AL and PCL; CNF = 19.2 wt % and AL = 5.00 wt %), CNF-PCL (CNF = 19.2 wt %), AL_x-PCL (AL = x = 1.00 or 5.00 wt %), and PCL. The electrical performance of the CNF-containing composites was measured, and conductivities of 14.0 ± 2, 22.0 ± 5, and 31.0 ± 6 S/m were observed for CNF_{AL}-PCL, CNF-AL_5-PCL, and CNF-PCL, respectively. CNF_{AL}-PCL and control films were degraded in phosphate buffer (2.00 mg/mL film/buffer) at 50 °C, and their average percent weight loss ($Wt_{avg\%}$) was recorded over time. After 3 h CNF_{AL}-PCL degraded to a $Wt_{avg\%}$ of 90.0% and had completely degraded after 8 h. This was considerably faster than CNF-AL_5-PCL, which achieved a total $Wt_{avg\%}$ of 34.0% after 16 days, and CNF-PCL, which was with a $Wt_{avg\%}$ of 7.00% after 16 days. Scanning electron microscopy experiments (SEM) found that CNF_{AL}-PCL has more open pores on its surface and that it fractures faster during degradation experiments which exposes the interior enzyme to water. An electrode made from CNF_{AL}-PCL was fabricated and attached to an AL_5-PCL support to form a fast-degrading thermal sensor. The resistance was measured over five cycles where the temperature was varied between 15.0−50.0 °C. The sensor was then degraded fully in buffer at 50 °C over a 48 h period.

INTRODUCTION

Recently, the concept of enzyme-mediated plastic degradation has received substantial attention from the scientific community[1−3] and the popular press[4−6] due to the development of a thermally stable poly(ethylene terephthalate) degrading enzyme (PETase),[7] which is more colloquially termed a "plastic eating enzyme".[5−8] Such enzymes generally fall into the "hydrolase" family (esterases, lipases, proteases, aminases, etc.), meaning that they typically mediate a hydrolysis reaction in the backbone of the plastic via a catalytic triad/oxyanion hole motif at the active site.[9] For polyester plastics with readily hydrolyzable backbones such as polycaprolactone (PCL), poly(lactic acid) (PLA), and polyhydroxybutyrate (PHB), enzymes such as common lipases, proteinase K, cutinases, and PHB depolymerase can facilitate degradation.[10,11] Delivery of the enzyme to the plastic can occur either externally or internally. External delivery methods usually dissolve the enzyme in a buffer which is placed in direct contact with the submerged plastic substrate.[10,12,13] Internal delivery methods generally refer to when the enzyme (immobilized or free) is physically embedded into the plastic,

Received: October 9, 2023
Revised: December 10, 2023
Accepted: December 11, 2023
Published: December 26, 2023

ACS Publications

Crown © 2023. Published by American Chemical Society

https://doi.org/10.1021/acs.biomac.3c01077
Biomacromolecules 2024, 25, 455−465

which is then degraded from the inside out when water/buffer activates the enzyme via diffusion into the matrix.[14−17] Enzymatic plastics recycling, which focuses on plastic end-of-life, utilizes external delivery methods to facilitate breaking down large amounts of plastic waste to produce monomers that can either be repolymerized or be converted into other specialty chemicals for future use.[18] Internal delivery methods have been mostly found in the literature as a method to speed up the plastics degradation process with regards to compostable packaging.[19,20] However, there have not been many examples of this method being used to improve the end-of-life for plastics used in other more high-value applications, e.g., electronics, which means that there is still an opportunity to explore this technology further.

Sensing and other electronic monitoring devices are ubiquitous in our everyday life and are especially important in industry where these instruments can be used to measure the freshness of produce in transit, environmental fluctuations, agriculture, and numerous other applications. Most of these devices contain metals (e.g., silver, copper) and fossil-based materials (e.g., printed circuit board), meaning that the end-of-life and toxicity of these devices can become an issue.[21−23] To solve this problem green or sustainable electronics are being developed to ameliorate these environmental issues.[24] Typical strategies include the substitution of metal-based conductive inks/materials with sustainably sourced carbon-based conductive materials, such as graphene or carbon nanomaterials, and replacing the body of the device/substrate with biodegradable polymers or natural materials to reduce its impact on the environment.[25−27] Recently, Beniwal et al. have showed that graphene-based carbon ink could be screen-printed onto a paper substrate to construct a humidity sensor with wireless communication.[28] Additionally, Tu et al. have showed that carbon-based inks could be printed onto dissolvable PVA/gelatin substrates for point-of-care testing.[29] Although these examples show advancement in green and biodegradable sensors, many applications require materials that are tear-proof and do not biofoul quickly but are guaranteed to degrade completely at the end of their service life. Biodegradable and compostable plastics are well-suited to tackle this problem; however, biodegradable plastics can suffer from slow or unreliable degradation.[30,31] Embedding hydrolytic enzymes into these biodegradable plastics would expedite the natural degradation process of these devices and provide a solution for this problem. Recently, Kwon et al. showed that silver inks compounded with PCL could be printed onto the surface of a PCL substrate embedded with lipase to produce sensors that degrade rapidly in the presence of warm water, allowing for the recovery and recycling of the silver ink.[32] Although this is a great stride forward for this technology, there are currently no systems that combine the fast-degrading properties of enzyme-embedded compostable plastics with environmentally benign conductive carbon-based materials.

Here, we demonstrate the development of a fast-degrading carbon-based conductive composite made from polycaprolactone and carbon nanofiber with immobilized lipase that rapidly breaks down in the presence of warm water. Carbon nanofibers (CNF) were chosen as an immobilization support and conductor due to their lower relative eco-toxicity compared to metal-based conductors and their potential to be manufactured from renewable/biobased resources (e.g., lignin).[25,33] Polycaprolactone (PCL) and Amano Lipase (AL) were selected due to polycaprolactone's biodegradability and compostability and Amano Lipase's thermal stability.[15] This represents the first time that hydrolytic enzymes have been immobilized onto environmentally benign carbon nanomaterials to form an all-in-one conductive biocatalyst with the express goal of degrading an encapsulating biodegradable plastic. Additionally, as proof-of-concept this novel composite material was used to fabricate a thermal sensor capable of degrading within a 48 h window under ideal conditions.

EXPERIMENTAL SECTION

General Information. PCL (M_n 45000, mp 56−64 °C, MFI 1.8 g/10 min at 80 °C, 44 psi), Amano Lipase PS from *Burkholderia cepacia* (≥10000 U/g, opt pH and temperature 7.0 and 50 °C, protein ∼1.0 wt %), 1-pyrenebutyric acid (PBA), 1-ethyl-3-(dimethylamino)-propyl)carbodiimide (EDC), carboxymethyl cellulose, monosodium phosphate (NaH_2PO_4), and disodium phosphate (Na_2HPO_4) were purchased from Sigma-Aldrich. Organic solvents, methanol and dimethyl sulfoxide (DMSO), were purchased from Merck. Sodium phosphate buffer (0.10 M, pH 7.5) was prepared via a standard recipe.[34] CNF (PR-24-XT-LHT-OX; avg diameter ∼150 nm, length ∼50−200 μm, aspect ratio ca. ∼300−1300, surface area ∼20−30 m^2/g) was procured from Pyrograf (Cedarville, OH). All materials were used as received except for polycaprolactone, which was cryoground to a fine powder (sieved, ≤300 μm). To ensure adequate heating and uniform mixing of samples during degradation experiments, an orbital incubating shaker (Lab Companion SI600R; Yuseong-gu, Daejeon, Korea) was used. Thermal pressing of sample films was performed on a hot press (Siempelkamp; Krefeld, DE), and sensing patterns were cut by laser scribing using a commercial CO_2 laser engraving machine (Makerspace G640L; NZ) with a laser power of 15 W and a scan rate of 100 mm/s.

Characterization. The electrical performance of CNF (pristine and functionalized) and subsequent PCL composites was measured using a multimeter (Limit 500). The resistances of commercial and functionalized CNFs were measured as a dried dispersion in carboxymethyl cellulose (1.0 wt %) over a distance of 20 mm to allow for direct comparison between treatment methods. The conductivities of PCL composite films (10 mm × 12 mm) were measured at a distance of 12 mm with silver ink at the interface to reduce contact resistance. For temperature sensing measurements real-time electrical resistance changes of sensor electrodes were recorded using an LCR meter (IM 3536 Hioki; Japan) with an applied voltage of 1.00 V. To measure the change in pH during degradation and titration experiments, a pH probe (Seven Compact, Mettler Toledo, Columbus, OH) equipped with an Ag/AgCl electrode was used. The surface and cross-sectional microstructures of CNFs (pristine and functionalized) and PCL-based composites (before/after degradation) were investigated via field emission scanning electron microscopy (FE-SEM) (JSM 6700 JEOL; Japan). Samples were sputter-coated with chromium (10.0 nm thickness) and analyzed at an accelerating voltage of 3.00 kV. To measure the crystallinity of PCL and PCL-based composites, differential scanning calorimetry (DSC) was performed in heat−cool−heat mode by a Discovery DSC (TA Instruments) equipped with a refrigerated cooling system. Samples (5.00 mg) were placed in a TZero aluminum pan under nitrogen (10 mL/min), and the following temperature cycle was used: equilibration at −80.00 °C; isothermal 5.00 min; ramp 10.00 °C/min to 80.00 °C; ramp 5.00 °C/min to −80.00 °C; isothermal 5.00 min; ramp 10.00 °C/min to 80.00 °C. Data from the second heating scan were used for the analysis. Thermogravimetric analysis (TGA) was performed on a TGA1-0329 instrument (TA Instruments, USA), using a heating ramp of 10.0 °C/min under a N_2 atmosphere. Liquid chromatography−mass spectrometry (LCMS) was performed using an Agilent Series 1290 HPLC (Agilent Technologies, Santa Clara, CA) equipped with a reverse phase C18 analytical column of 150 mm × 3.0 mm and 2.7 μm particle size (Poroshell 120 EC-C18). Chemical surface analysis was performed

https://doi.org/10.1021/acs.biomac.3c01077
Biomacromolecules 2024, 25, 455−465

Table 1. Composition and Conductivity of PCL/CNF-Based Composites[a]

sample	PCL (wt %)	CNF (wt %)	CNF_{AL} (wt %)	AL powder (wt %)	activity (U/100 mg)	conductivity (S/m)
CNF_{AL}-PCL	80.0		20.0		14.4	14.0 ± 2
CNF-AL_5-PCL	75.8	19.2		5.02	50.0	22.0 ± 5
CNF-PCL	81.0	19.2				31.0 ± 6
PCL	100					

[a]Values rounded to three significant figures.

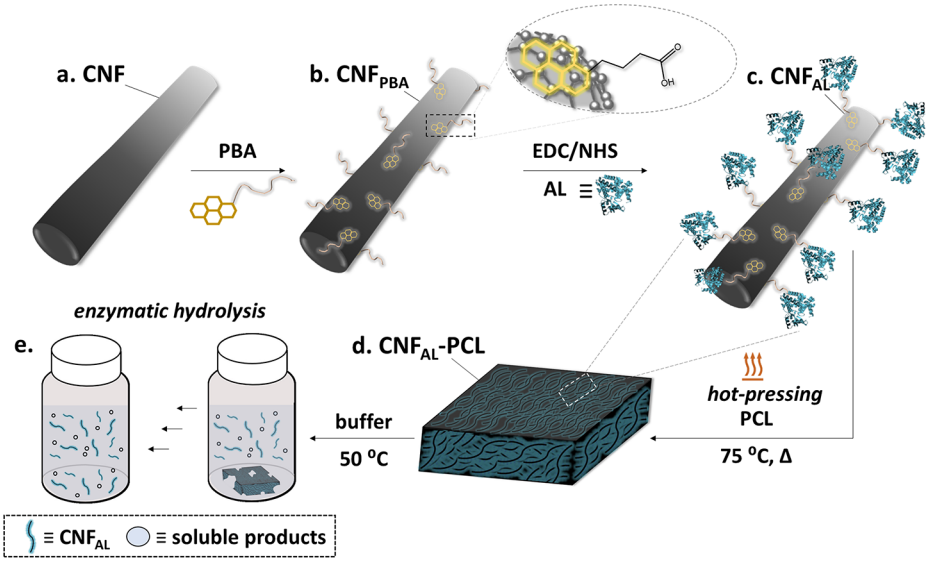

Figure 1. Graphical representation of the manufacturing process and compounding of a fast-degrading conductive composite. (a) Pristine carbon CNF is first reacted with PBA to form (b) CNF_{PBA}. CNF_{PBA} is then coupled to AL via EDC/NHS coupling to form (c) CNF_{AL}. CNF_{AL} is then hot pressed at 60 °C with PCL to form the fast-degrading conductive composite (d) CNF_{AL}-PCL and conductive composite. (e) Enzymatic hydrolysis of CNF_{AL}-PCL via embedded CNF_{AL} in buffer at 50 °C with agitation.

using a Kratos AXIS DLD X-ray photoelectron spectrometer (XPS) equipped with a hemispherical electron energy analyzer. For sample excitation, a monochromatic Al Kα source (1486 eV, 150 W) was used, and survey scans were collected (160 eV pass energy), followed by core level scans for O, N, and C. The analysis chamber was evacuated to pressures in the range of 1.3×10^{-9} mbar. Data analysis was performed using the Casa XPS software; relative sensitivity factors for the elements were used as supplied with the instrument. For electrically conductive samples, no charge correction was applied. Nonconductive samples were referenced to 284.8 eV for their C 1s peak. Background correction was done using Shirley backgrounds. For the core scan data, graphite was used as the reference material. Enzyme activity measurements were performed using a standard *p*-nitrophenol assay at room temperature.

Immobilization of Lipase (AL) onto CNF. *CNF_{PBA}*. The immobilization of lipase on to CNF was adapted and modified from the literature.[35] CNFs (1.00 g) were dispersed in DMSO (35.0 mL) and sonicated for 1 h at 25 °C. The dispersion was then transferred to a 50.0 mL centrifuge tube where 1-pyrenebutyric acid (PBA) (1.18 g) and an additional 5.00 mL of DMSO were added. The mixture was shaken for 3 h (25 °C, RCF = 1.05*g*) and then centrifuged for 10 min (18 °C, RCF = 3184*g*). The supernatant was then decanted, and the remaining black solids were washed and centrifuged with methanol and then water. After washing, the remaining solids were freeze-dried and recovered. The total weight fraction of bound PBA was found to be 10.0% by titration, Yield 1.10 g.

CNF_{AL}. PBA-functionalized CNFs (0.764 g) were dispersed in phosphate buffer (90.0 mL, pH 7.2, 50.0 mM) and sonicated for 1 h at 25 °C. Then, additional buffer (20.0 mL) and EDC (3.34 g) were added, and the mixture was shaken for 30 min (25 °C, RCF = 1.05*g*). The reaction mixture was then centrifuged for 10 min and decanted, and the remaining black solid was washed with additional buffer via centrifugation. The activated black solid was again dispersed in fresh phosphate buffer (20.0 mL, pH 6.5, 50.0 mM), and 75.0 mL of lipase solution in buffer (9000 U, pH 6.5) was added. The mixture was then shaken for 30 min (RCF = 1.05*g*), centrifuged, washed with methanol and then water, and freeze-dried. The immobilized material was found to have an activity of 0.720 U/mg, and the immobilization yield was found to be 4.60% (see the Supporting Information). Yield 0.514 g.

General Procedure for the Preparation of Fast-Degrading Conductive Composites. CNF_{AL}-PCL. Ground PCL was dried at 40 °C in a vacuum oven for 2 days and then manually mixed with AL-functionalized CNF (CNF_{AL}) in a PTFE-coated vessel at 75 °C, maintaining a 20.0 wt % ratio of CNF_{AL} to PCL. The compounded mixtures were then hot pressed between PTFE-coated steel plates at 75 °C for 1 min at 50.0 kN, followed by 1 min at 30.0 kN to a thickness of 600 μm. To achieve a smooth surface, all films were pressed and repressed at least two times. An additional film CNF-AL_5-PCL, containing unimmobilized (free) AL powder, pristine CNF, and PCL, and control films containing CNF-PCL (no enzyme), AL_x-PCL (x = 1.00, 5.00%; no CNF), and pure PCL were also fabricated (see Table 1 and the Supporting Information for weight ratios and compositions). Weight percentages for AL are based on the unpurified powder. All films were then analyzed by FE-SEM, DSC, and TGA and for their electrical performance. Samples were stored in a desiccator prior to use.

Degradation of Fast-Degrading Conductive Composites. CNF_{AL}-PCL film and control samples (40.0 mg) were placed into glass scintillation vials containing phosphate buffer (2.00 mg/mL film to buffer; pH 8.0, 0.100 M) and capped with a PTFE-lined screw cap. The samples were placed in an orbital incubator shaker and maintained at a temperature of 50 °C and shaken at RCF = 1.05*g* for up to 24 days or until full degradation. Samples of each film were prepared in triplicate for each time point observed and consumed. At the end of each time point the degradation mixture was carefully

https://doi.org/10.1021/acs.biomac.3c01077
Biomacromolecules 2024, 25, 455−465

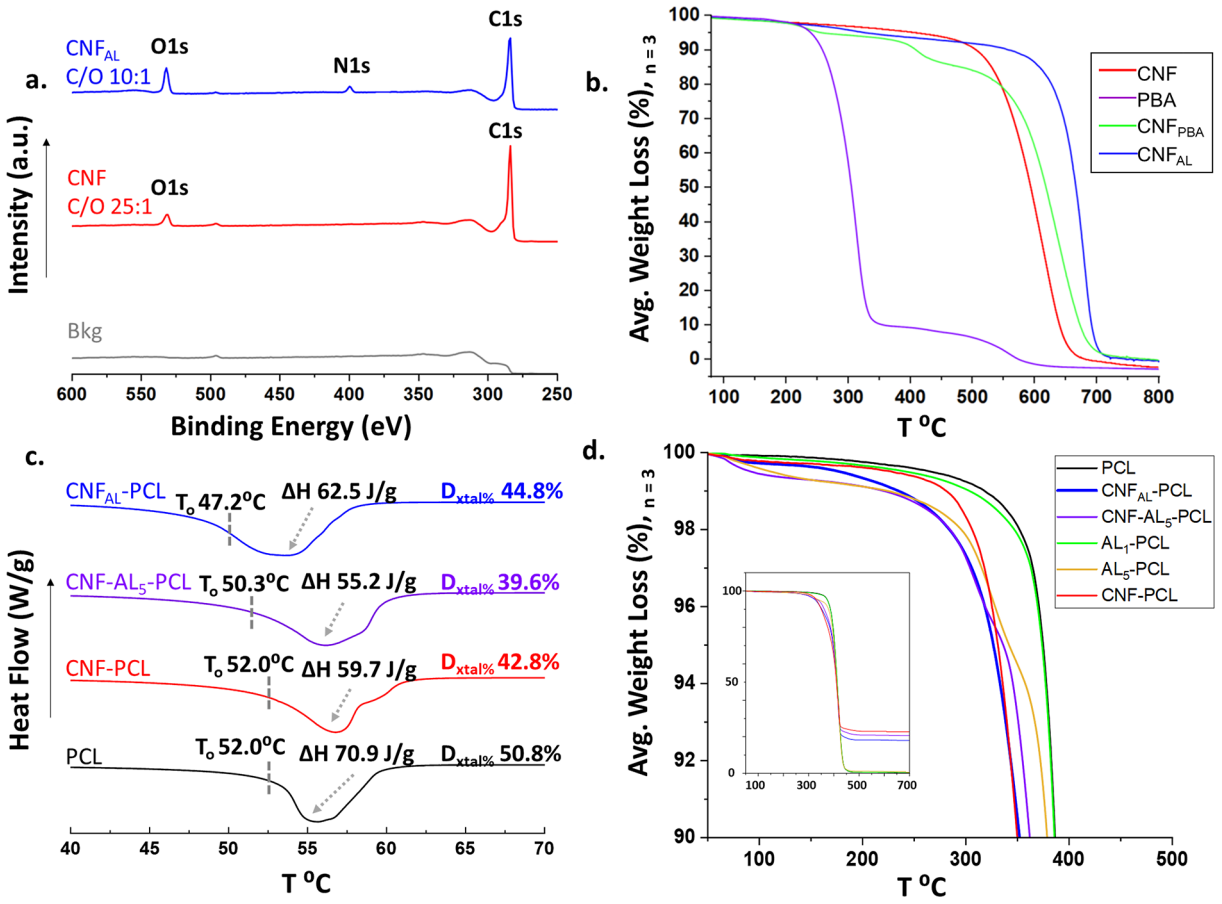

Figure 2. (a) XPS of AL immobilized carbon nanofibers (CNF_{AL}) and pristine CNF. (b) TGA showing the average weight loss percentage of CNF_{PBA}, CNF_{AL}, pristine CNF, and PBA. (c) DSC showing the percent crystallinity ($D_{xtal\%}$), melting onset temperature (T_o), and heat of fusion (ΔH) of CNF_{AL}-PCL, CNF-AL_5-PCL, CNF-PCL, and PCL composite films. (d) TGA showing the average weight loss percentage of the composite films CNF_{AL}-PCL, CNF-AL_5-PCL, and the positive and negative controls.

transferred and centrifuged at RCF = 3184*g* for 10 min. The supernatant was decanted, freeze-dried, and analyzed by LCMS, while the collected residue was washed repeatedly with deionized water and recollected by centrifugation, freeze-dried, and weighed to obtain the total percent weight loss ($Wt_{avg\%}$). Undegraded plastic film residue from selected time points were then analyzed by FE-SEM.

Degradation of Fast-Degrading Thermal Sensor. A thermal sensor composed of [CNF_{AL}-PCL/AL_5-PCL] was placed into a 200 mL beaker, and phosphate buffer (2.00 mg/mL film to buffer; pH 8.0, 0.100 M) was added. Then the beaker was tightly secured and covered with aluminum foil. The bottles containing the sensor and buffer solution were then placed in an orbital incubator shaker at 50 °C (RCF = 1.05*g*) and were degraded over a period of 48 h.

RESULTS AND DISCUSSION

In this study we describe the preparation, fabrication, and enzyme-mediated rapid degradation of environmentally benign conductive thermoplastic composites. To prepare these materials, CNFs were functionalized with a polyester-degrading lipase, AL, and these enzyme-coated fibers were then compounded with the biodegradable polyester, PCL, which serves as the thermoplastic matrix to be enzymatically degraded (Figure 1a–e). Additionally, to demonstrate the viability of these composites for use in electronic sensing devices, a thermal sensor was fabricated, characterized, and finally degraded as a proof-of-concept.

Immobilization of AL onto CNF. A modified procedure[35] from Min et al. was used to immobilize AL onto CNF via an intermediate linking step with 1-pyrenebutyric acid (PBA). Pristine CNF was initially reacted with PBA through supramolecular $\pi-\pi$ interactions between the surface of the CNF and the aromatic pyrene system (Figure 1a,b). To measure the amount of PBA immobilized onto CNF, a titration was performed by dispersing the resultant CNF_{PBA} material into dilute NaOH and titrating the deprotected COO^- groups with dilute HCl (Table S1). From the titration it was determined that CNF_{PBA} contained ~10.0 wt % PBA. To complete the immobilization of AL onto CNF, CNF_{PBA} was then reacted with AL via a standard EDC coupling to form the conductive biocatalyst CNF_{AL} (Figure 1c).[36] The activity of the resulting immobilized CNF_{AL} material was found to be 0.720 U/mg after reaction with *p*-nitrophenol, and the calculated immobilization yield was found to be 4.10%.

$$(a)\ \text{immobilization yield} = \frac{\text{immobilized activity}}{\text{starting activity of free enzyme}}$$

Further characterization of CNF_{AL} was also performed using X-ray photoelectron spectroscopy (XPS) (Figure 2a). Analyzing the resulting peaks from pristine CNF and CNF_{AL} both show a strong C 1s peak from 284 to 290 eV and a slightly weaker peak for O 1s at ~531 eV; however, only CNF_{AL} shows a peak for N 1s. The C/O ratios for CNF and CNF_{AL} are 25:1 and 10:1, respectively, and the C/N ratio for CNF_{AL} is 33:1, which is in line with the enzyme being immobilized to the substrate as AL is the only apparent nitrogen source. Thermal

https://doi.org/10.1021/acs.biomac.3c01077
Biomacromolecules 2024, 25, 455–465

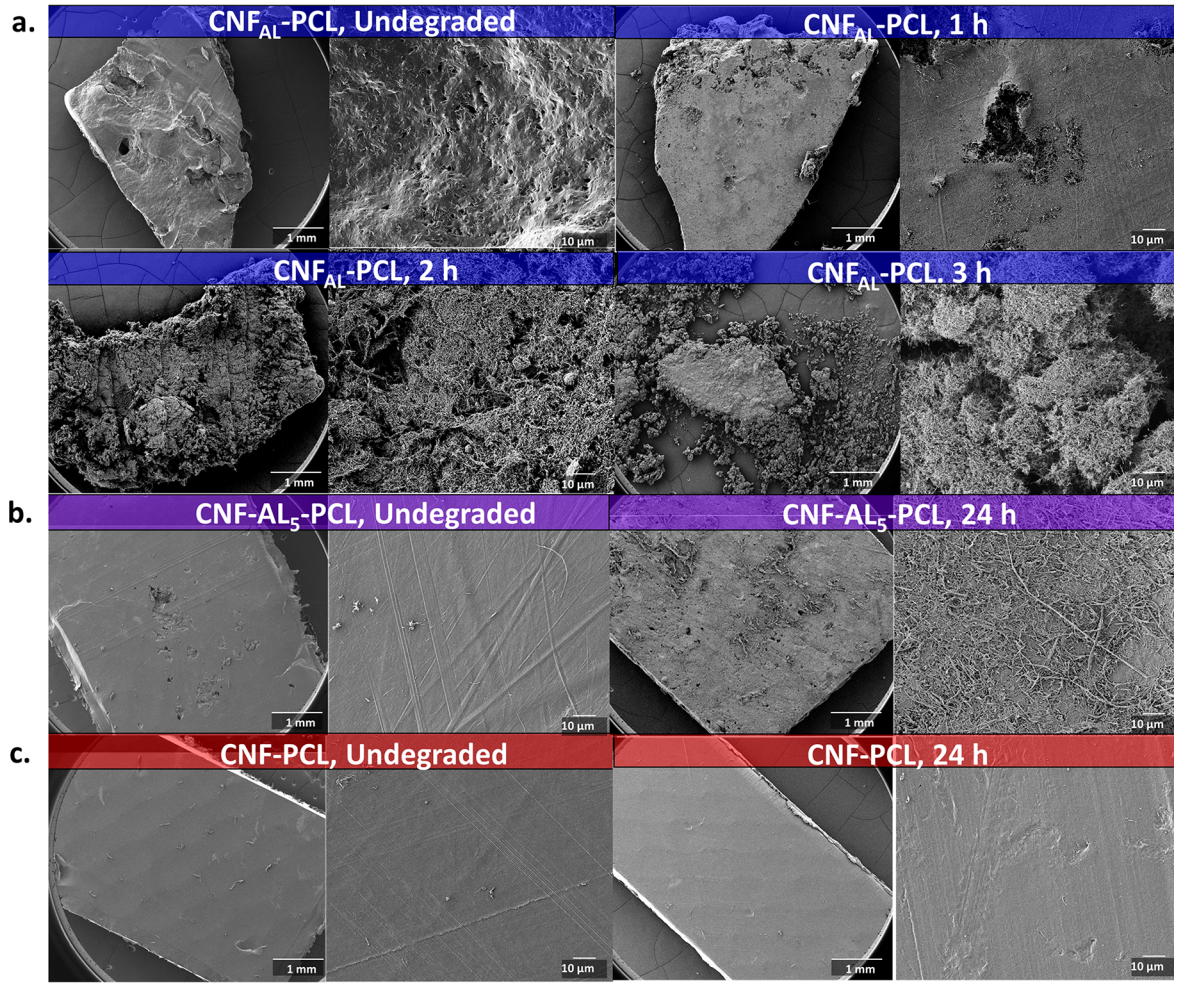

Figure 3. (a) Scanning electron microscopy (SEM) images of CNF$_{AL}$-PCL undegraded film and after 1, 2, and 3 h of degradation. (b) Images of CNF-AL$_5$-PCL and (c) CNF-PCL undegraded film and after 24 h of degradation.

gravimetric analysis (TGA) was also conducted on CNF, PBA, CNF$_{PBA}$, and CNF$_{AL}$ (Figure 2b). The degradation curve of pristine CNF shows a 98.0% weight loss between 550−650 °C, which is attributed to the degradation of the CNF material itself. The weight loss data of CNF$_{AL}$, however, show an initial ∼5.0% loss between ∼300−400 °C and then a 95.0% weight loss between ∼650−700 °C. From analyzing the other samples this 5.00% loss is possibly due to hydrogen bound water or other impurities as it is also present in CNF$_{PBA}$, but not in pristine CNF. In CNF$_{PBA}$, the degradation of PBA occurs between 400−500 °C, as shown by an ∼10.0% weight loss which matches well with titration experiments. This weight loss is not present in CNF$_{AL}$, meaning that bound PBA is stabilized and protected via conjugation with the enzyme. Additionally, the degradation of CNF is delayed by about ∼100 °C due to this conjugation, as compared with pristine CNF. As for the electrical performance of CNF$_{AL}$, it was found to have a resistance of 600 ± 126 Ω compared to 575 ± 140 Ω for pristine CNF, both determined using an equal amount of sample dispersed over an equal surface area, to allow direct quantitative comparison (Table S2). Analyzing the data there appears to be no significant change in resistance of CNF post functionalization.

Fabrication of Fast-Degrading Conductive Composites. Composites containing CNF and PCL with no AL were first compounded and hot-pressed to a thickness of 600 μm at different weight percentages of CNF in PCL (5.00, 10.0, 15.0, 20.0, and 30.0 wt %), and the conductivity of each material was measured (Figure S1). This was to determine the minimum amount of CNF needed to ensure the highest level of performance, while maintaining structural integrity. It was found that 20.0% CNF was the maximum amount of CNF that could be added to the composite before the conductivity begins to level off, producing diminishing returns (Figure S1a). Once this had been determined, composites containing CNF$_{AL}$ and PCL were fabricated in a similar manner to produce the fast-degrading conductive thermoplastic material, CNF$_{AL}$-PCL. The total composition of CNF$_{AL}$-PCL was found to be 20.0% CNF$_{AL}$ and 80.0% PCL with a total activity per weight added of 14.4 U/100 mg of composite (Table 1). To understand how immobilization of AL effects the degradation of the material, another set of composites were fabricated containing CNF, PCL, and unimmobilized AL powder, CNF-AL$_x$-PCL (x = 1.00 or 5.00 wt % AL powder; 10.0 and 50.0 U/100 mg, respectively). These compositions were chosen as it has been previously demonstrated that these percentages of AL powder in PCL with no CNF present are very effective at degrading PCL;[15] however, preliminary degradation studies showed no degradation activity present in CNF-AL$_1$-PCL after 24 days, so the study was continued only using CNF-AL$_5$-PCL. In addition to CNF$_{AL}$-PCL and CNF-AL$_5$-PCL, an assortment of positive and negative controls was also fabricated including CNF-PCL,

https://doi.org/10.1021/acs.biomac.3c01077
Biomacromolecules 2024, 25, 455−465

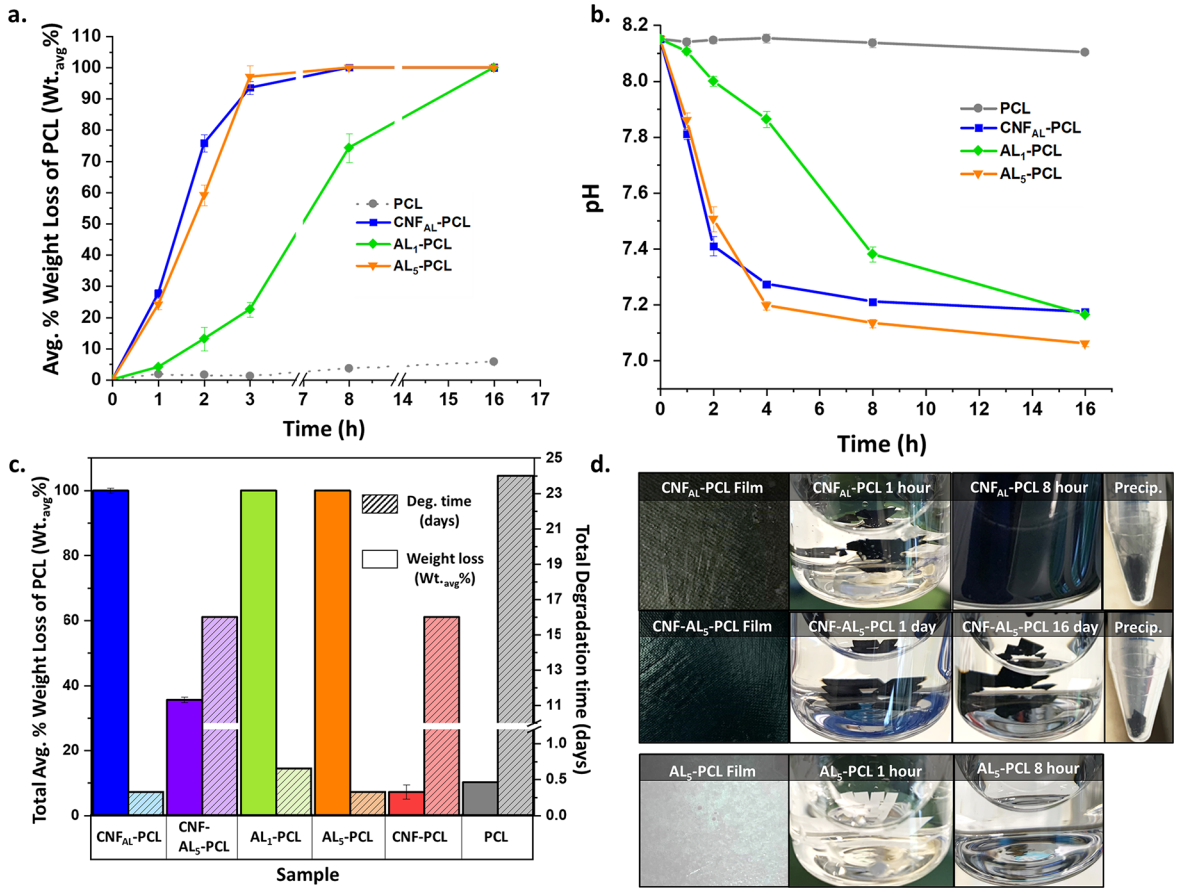

Figure 4. (a) Average percent weight loss ($Wt_{avg\%}$) of CNF_{AL}-PCL and control films at 50 °C, RCF = 1.05*g*, over 16 h. (b) Change in pH of buffer during 16 h degradation of CNF_{AL}-PCL and control films. (c) Histogram depicting the time (Deg. time) that each composite film takes before no further degradation is observed and total average weight loss percent achieved during that period. (d) Pictures of CNF_{AL}-PCL, CNF-AL_5-PCL, and AL_5-PCL during various stages of the degradation process.

where no AL is present, and AL_x-PCL (x = 1.00 or 5.00 wt % AL powder; 10.0 and 50.0 U/100 mg, respectively), where no CNF is present (see Tables 1 and S3 for composition data). The conductivity of PCL-based CNF composites decreases with the addition of AL; this is an expected result as AL is not an electrically conductive material. Experimental measurements demonstrate that CNF-PCL has the highest conductivity at 31.0 ± 6 S/m, and CNF_{AL}-PCL and CNF-AL_5-PCL have a similar conductivity at 14.0 ± 2 and 22.0 ± 5 S/m, respectively (Table 1).

DSC and TGA were performed to investigate the thermal properties of the composites (Figure 2c,d). PCL is known to exist in a variety of phases, including fully crystalline and plastic crystal mesophases,[37] the presence and extent of which depend on the processing conditions. For pure PCL both the degree of crystallinity and onset of melting temperature (50.8% and 52.0 °C, respectively) are highest among all the composites, except for CNF-PCL where the onset of melting temperature is the same. The melting behavior of pure PCL is also characterized by a single peak, indicating the presence of one predominant type of crystallites. By contrast, CNF-PCL and CNF-AL_5-PCL display melting transitions that clearly represent two distinct processes and, correspondingly, the presence of two different types of crystalline phases. The total degree of crystallinity is lower for both (42.8% and 39.6%, respectively), while the onset of melting is shifted down by a few °C. Because both composites contain nonfunctionalized CNF, it is likely that this change in the PCL matrix is caused by the influence the bare CNF surfaces have on the polymer crystallization (e.g., through nucleation and/or stabilization of a different phase). CNF_{AL}-PCL, however, shows a single melting peak with an even lower onset temperature and an intermediate degree of crystallinity (44.8%). Because the CNF present in this material are decorated with enzyme, their surface properties can be expected to significantly differ from nonfunctionalized CNF, which in turn is likely to lead to a different effect on the crystallization process of the PCL. A different phase composition of the crystalline domains in the various composites can be assumed to be the reason for the qualitatively observed brittleness of CNF_{AL}-PCL versus the other composites. Thermal gravimetric analysis (TGA) revealed that the degradation profiles observed for all composites aligns well with their reported compositions (Figure 2d). All composites containing CNF report an ∼75.0−80.0% weight loss between 350−400 °C, which accounts for the loss of the PCL polymer matrix. CNF_{AL}-PCL and CNF-PCL also share a similar degradation profile except for a small weight loss for CNF_{AL}-PCL between 175−300 °C, which can be reasonably attributed to either hydrogen bound water and/or PBA and immobilized AL. Similarly, CNF-AL_5-PCL and Al_5-PCL both show an ∼5.00% weight loss between 100−300 °C which can be attributed to the loss of free AL powder. To investigate the surface and cross-sectional morphologies, SEM images were captured for all composites

https://doi.org/10.1021/acs.biomac.3c01077
Biomacromolecules 2024, 25, 455−465

prior to degradation. The surface of undegraded CNF_{AL}-PCL (Figure 3a) is rather uneven in nature, and it is evident at high magnification that CNFs immobilized with AL are present on the surface forming a patchwork-like pattern in the plastic. In contrast, CNF-AL_5-PCL and CNF-PCL seem to have a far smoother contiguous surface with little to no CNF (pristine) present even at high magnification (Figure S2). Analyzing the cross-sectional images, CNF is visible in all three composites, and there is no indication of increased bundling, clustering, or alignment of CNF. However, it is noted that the polymer matrix of CNF-PCL and CNF-AL_5-PCL displays a grainy structure in cross section which was also found in pure PCL (Figure S3). It was absent, however, in CNF_{AL}-PCL, which correlates well with DSC results as CNF_{AL}-PCL is shown to have a different crystalline phase that results in a lower melting temperature. Additionally, AL was also found to be well distributed throughout the composite as evidenced via fluorescence microscopy with fluorescein tagged AL (Figure S4). Dynamic mechanical thermal analysis (DMTA) was undertaken to quantify the difference in mechanical properties between the composites; however, due to the brittleness of CNF_{AL}-PCL, the results were inconclusive. Although CNF_{AL}-PCL is rather brittle, this does not prevent the material from being deployed in small sensors or other electronic devices that are fit-for-purpose and that are not subject to high mechanical loads.

Degradation Trials. To test the degradation capabilities of CNF_{AL}-PCL and CNF-AL_5-PCL, under ideal conditions, 40.0 mg of rectangular films with a thickness of ∼600 μm were cut and submerged in basic phosphate buffer (plastic to buffer ratio 2.00 mg/mL). The films were heated and shaken at 50 °C and 2 RCF = 1.05g. This procedure was also performed for the positive controls AL_1-PCL and AL_5-PCL and for negative controls CNF-PCL and PCL. Sacrificial samples were made for each selected time point to measure how the films degrade over time, and the films were kept under degradation conditions for a maximum of 24 days or until full degradation and dissolution of degradation products occurred. For degraded samples containing CNF, special care was taken to disambiguate liberated CNF from undegraded PCL film by centrifuging the terminal samples after each time point measured. PCL film is denser than CNF and sinks to the bottom of the centrifuge tube, while CNF floats to the top as a finely dispersed particulate. As the degradation experiments progressed, it was immediately evident that the degradation activity between CNF_{AL}-PCL and CNF-AL_5-PCL occurred on vastly different time scales with CNF_{AL}-PCL degrading rapidly in a matter of hours while full degradation of CNF-AL_5-PCL failed to occur even after 24 days. Figures 4a and S5 show the average percent weight loss of PCL ($Wt_{avg\%}$) for CNF_{AL}-PCL, the positive controls, and PCL over a 16 h period. Within the first hour the $Wt_{avg\%}$ for CNF_{AL}-PCL was around 30.0%, and astonishingly after the third hour it was at 90.0% total PCL weight loss. The degradation profile of CNF_{AL}-PCL tracks well with the positive control AL_5-PCL, which is even more impressive as CNF_{AL}-PCL has a lower activity per mass ratio than AL_5-PCL, 14.0 U vs 50.0 U mg present per 100 mg of composite, respectively, and because AL_5-PCL was specifically fabricated to be a fast-degrading formulation. In total, it takes CNF_{AL}-PCL and AL_5-PCL 8 h to fully degrade, while AL_1-PCL, which has an activity of 10.0 U/100 mg of composite, takes 16 h for full disintegration and dissolution. To obtain a more complete understanding of what degradation products were formed during this experiment, aliquots of the supernatant were analyzed by LCMS after 3 h for CNF_{AL}-PCL, AL_1-PCL, and AL_5-PCL (Table 2). For CNF_{AL}-PCL it was found that most degradation products had molecular weights below ∼1000 Da with 63.0% between ∼500−1000 Da and 18.4% below ∼500 Da. Only a small percentage of products, 18.7%, were found to be between ∼1000−2000 Da. As for the positive controls, the fastest degrading film AL_5-PCL was found to have most of its degradation products below ∼500 Da, 66.0%, with only 33.2% between ∼500−100 Da and <1.00% over 1000 Da.

Table 2. Percent Distribution of Molecular Weights (D%) after Degradation (3 h)[a]

sample	<500 (Da)	500−1000 (Da)	1000−2000 (Da)
CNF_{AL}-PCL	18.4	63.0	18.7
AL_1-PCL	16.2	58.0	25.8
AL_5-PCL	66.0	33.2	0.860

[a]Values rounded to three significant figures.

AL_1-PCL showed a degradation product molecular weight distribution more similar to CNF_{AL}-PCL after 3 h with the majority of its products between ∼500−100 Da. In addition to the 50 °C degradation experiments, CNF_{AL}-PCL composites were also degraded at 30 °C (Figure S6b) to understand how AL performed below its optimum temperature. It was found that after 14 days CNF_{AL}-PCL composites of a similar size showed a $Wt_{avg\%}$ of 50.0%, which is still much faster than CNF-AL_5-PCL at 50.0 °C. When PCL is hydrolyzed by AL, soluble acidic oligomers and 6-hydroxyhexanoic acid are produced, which lower the pH of the overall degradation media. In addition to measuring the $Wt_{avg\%}$ for CNF_{AL}-PCL and the control films, the pH was also monitored during the 16 h degradation period (Figure 4b). The pH traces for CNF_{AL}-PCL and AL_5-PCL also track similarly with a pH drop around ∼0.3 units after the first hour and ∼0.6 units after the second hour; after 2 h the drop in pH begins to slow down and eventually levels off after 8 h. For AL_1-PCL this decrease also tracks the degradation of the film with a slow drop in pH for the first 4 h and then a much larger drop around 8 h and eventually falling to the level of CNF_{AL}-PCL and AL_5-PCL (Figure 4b).

SEM images were also taken of CNF_{AL}-PCL and CNF-AL_5-PCL at different points during degradation to analyze the surface and cross-sectional morphologies of actively degrading films (Figures 3a,b and S2). SEM images of the fast-degrading CNF_{AL}-PCL were taken every hour during the first 3 h of degradation, and images of CNF-AL_5-PCL were taken after the first 24 h of degradation. Analyzing the images of CNF_{AL}-PCL during the first hour of degradation, it was already apparent that the volume of PCL was beginning to lessen as the presence of CNF fibers becomes exaggerated at the surface. Additionally, large gaps in the film, which are formed when the PCL matrix is degraded from the inside out, via an embedded enzyme, are beginning to form after the second hour. It is surmised that these large gaps greatly increase the speed of degradation as new channels are formed throughout the plastic, giving rise to the activation of deeply embedded AL by water. After the third hour the PCL seems to have mostly degraded demonstrating a total loss in integrity in the film. This contrasts with the images of the CNF-AL_5-PCL film, which were taken after 24 h, that appear to only be slightly eroded at the surface. Figure 4c shows the amount of time that

https://doi.org/10.1021/acs.biomac.3c01077
Biomacromolecules 2024, 25, 455−465

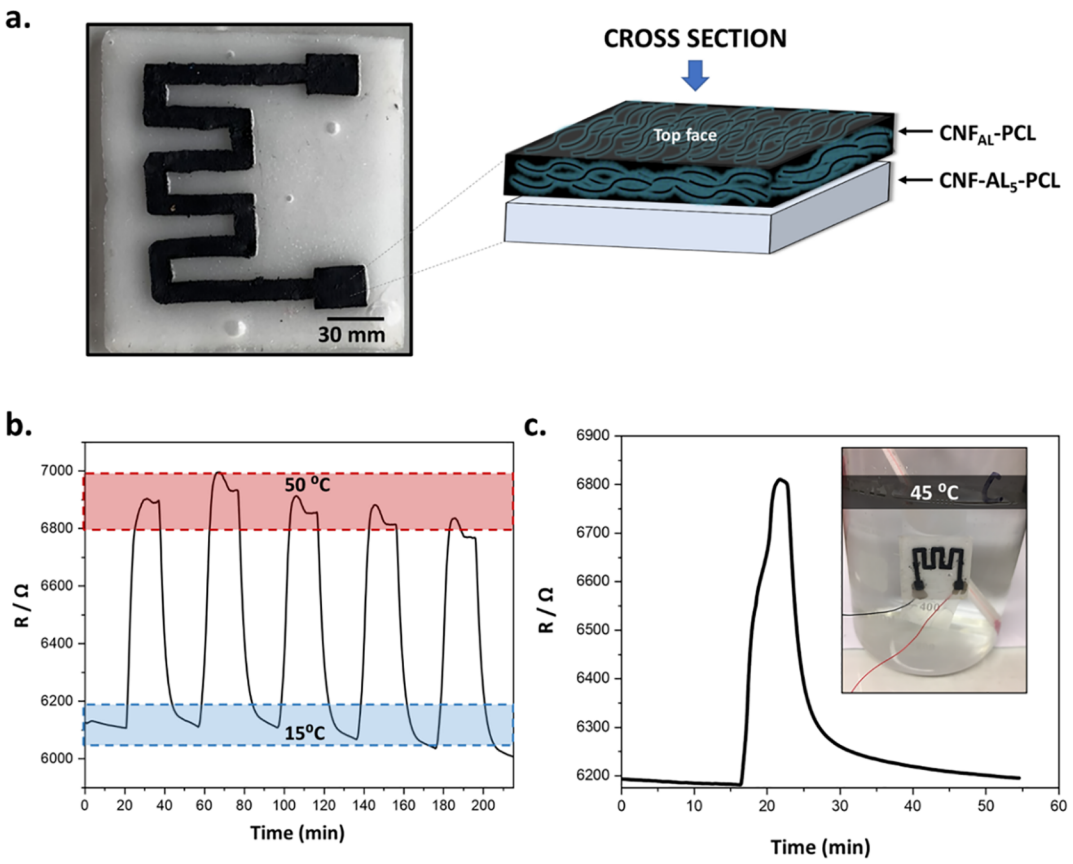

Figure 5. (a) Image and diagram of fast-degrading thermal sensor. (b) Total resistance change of the thermal sensor during five cycles of heating and cooling at 20 min intervals between 15−50 °C. (c) Total resistance change measured when the thermal sensor was placed into contact with a heated beaker of water at 45 °C.

each composite film takes before no further degradation is observed and the total weight loss achieved during that period. CNF-AL$_5$-PCL degrades for 16 days until a final weight loss average of 34.0% is achieved, while the negative controls CNF-PCL and PCL also take 16 days to reach a final weight loss of 7.00% and 9.00%, respectively. The drastic difference in degradation speed between CNF$_{AL}$-PCL and CNF-AL$_5$-PCL can be majorly attributed to the lack of open channels on the surface of CNF-AL$_5$-PCL that allow for water to enter the plastic matrix, thereby "activating AL". Another major reason is that CNF$_{AL}$-PCL is more brittle than CNF-AL$_5$-PCL and has a higher propensity to fracture during the degradation process exposing more surfaces to an aqueous environment speeding up degradation of the plastic. CNF-PCL was found to be the lowest performing composite film overall which suggests that the addition of the hydrophobic pristine CNF to the PCL matrix may reduce the efficiency of the unmediated hydrolysis reaction, which could also be contributing to the poor performance of CNF-AL$_5$-PCL.

Fabrication, Testing, and Degradation of Thermal Sensor. To examine the applicability of these fast-degrading materials, a thermal sensor was fabricated using a CNF$_{AL}$-PCL electrode and an AL$_5$-PCL support material; AL$_5$-PCL was chosen as support as it is the fastest-degrading nonconductive composite. The sensor electrodes were prepared by laser scribing pressed films of CNF$_{AL}$-PCL into a serpentine pattern (Figure S8) using a CO_2 laser cutting machine at room temperature. Additionally, a square support (30 mm^2) made from AL$_5$-PCL was also cut via laser scribing and fused to the CNF$_{AL}$-PCL electrode via hot pressing at 55 °C to form the sensor (Figure 5a).

To test the performance of the fast-degrading thermal sensor, the device was placed into an environmental testing chamber (30% relative humidity (RH)), and the temperature was cycled from 15 to 50 °C five times with 20 min resting intervals at each temperature while the overall resistance was monitored (Figure 5b). From the cycling experiments the sensor was found to display a significant and repeatable electric response between 15−50 °C, indicating a positive temperature coefficient (PTC). Semicrystalline thermoplastic polyesters, such as PCL, can be used as thermal sensing substrates due to the transformation of the crystalline phase to the amorphous phase as the temperature changes.[38] When CNF$_{AL}$-PCL is heated close to its melting point (around 50 °C), the crystalline phase of PCL becomes amorphous, which results in volumetric expansion and enlarges the distance between the CNF fibers. Once the conductive composite is cooled down, the polymer begins to recrystallize, which then reforms the conductive pathways. During this experiment only a minor change in performance was observed between the first and fifth cycle with the line shape conserved throughout; however, a limited amount of baseline drift was noted. Clearly optimization is still required to increase the sensitivity and in particular stability over time of this initial proof-of-concept device. The sensor was also tested outside of the environmental chamber to observe its behavior in nonideal conditions by attaching and detaching it to a beaker of warm water at 45 °C and measuring its response (Figure 5c). As the sensor was

https://doi.org/10.1021/acs.biomac.3c01077
Biomacromolecules 2024, 25, 455−465

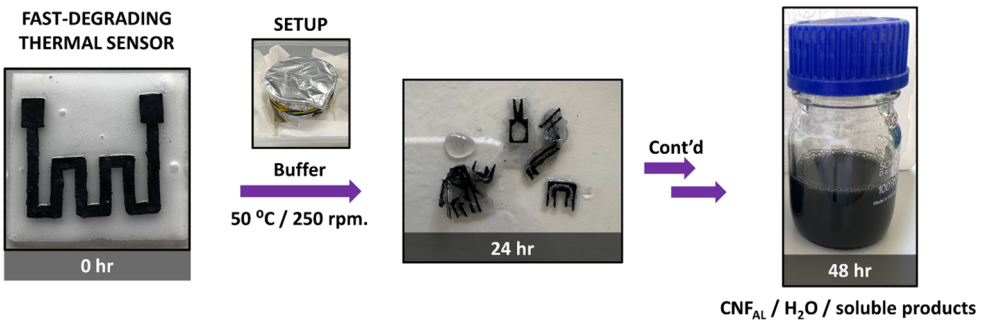

Figure 6. Images of the fast-degrading thermal sensor over a 48 h degradation period. The films are placed in a beaker, filled with buffer, covered, and placed in an incubator shaker at 50 °C and RCF = 1.05*g* (setup). After 48 h no film is observed, and only CNF, water, and soluble degradation products remain after centrifugation.

placed onto the warm beaker of water (t = ∼17 min), it showed an immediate response to the change in temperature reaching a maximum change in overall resistance within ∼3 min. When it was detached, it initially showed an immediate and steep drop in resistance; however, it took far longer for it to relax back to the original value. This long equilibrium time was also noted when the sensor was monitored in the environmental chamber during repeated heating and cooling cycles (Figure S9).

The degradability of the thermal sensor was then tested under ideal laboratory conditions. The sensor was placed into a glass beaker, suspended in buffer, covered, and placed into an orbital incubator shaker at 50 °C and RCF = 1.05*g* (Figure 6). This temperature was chosen as it is listed as the optimum temperature for AL from the manufacturer; however, the enzyme is active at a wide range of temperatures and has been shown to degrade PCL while embedded even at 37 °C.[15] After 24 h the AL$_S$-PCL support had completely degraded with only small pieces of the CNF$_{AL}$-PCL electrode left over. The remnants of the electrode were then allowed to react in the same buffer solution for an additional 24 h (total 48 h) where it fully degraded, only leaving finely suspended CNF$_{AL}$ and soluble organic degradation products (Figure 6) as evidenced by centrifugation of the resultant solution.

SUMMARY AND CONCLUSIONS

Here we report the development of a fast-degrading conductive thermoplastic made from environmentally benign materials and the fabrication of a thermal sensor from this thermoplastic that rapidly degrades in the presence of warm water. To produce this material, we have shown that AL can be successfully immobilized onto carbon nanofibers and compounded with PCL, retaining its activity, to produce the fast-degrading material CNF$_{AL}$-PCL. During degradation trials it was demonstrated that CNF$_{AL}$-PCL greatly outperformed the positive control CNF-AL$_S$-PCL where AL was not immobilized onto CNF. This difference in performance was attributed to the fact that CNF$_{AL}$-PCL has more channels on the surface of the film, and it fractures more easily during the degradation process, allowing for more water to penetrate the polymer matrix and activate the immobilized lipase. It was also demonstrated that CNF$_{AL}$-PCL can be fabricated into an electrode and integrated with other components to produce a proof-of-concept thermal sensor that can be degraded completely in 48 h in the presence of warm water. Although more work is needed to further optimize these types of devices and reduce the long relaxation times, the material CNF$_{AL}$-PCL is believed to be a promising environmentally benign solution for green electronics applications in the future.

ASSOCIATED CONTENT

Supporting Information

The Supporting Information is available free of charge at https://pubs.acs.org/doi/10.1021/acs.biomac.3c01077.

Additional experimental methods, CNF characterization, SEM images of composites, composite weight percent information, electrical performance, LCMS, and sensor testing (PDF)

AUTHOR INFORMATION

Corresponding Author

Angelique F. Greene − *Te Papa Tipu Innovation Park, Rotorua, New Zealand 3010*; orcid.org/0000-0003-2715-8660; Phone: +64 7 343 5864; Email: angelique.greene@scionresearch.com

Authors

Robert Abbel − *Te Papa Tipu Innovation Park, Rotorua, New Zealand 3010*

Alankar A. Vaidya − *Te Papa Tipu Innovation Park, Rotorua, New Zealand 3010*

Queenie Tanjay − *Te Papa Tipu Innovation Park, Rotorua, New Zealand 3010*

Yi Chen − *Te Papa Tipu Innovation Park, Rotorua, New Zealand 3010*

Regis Risani − *Te Papa Tipu Innovation Park, Rotorua, New Zealand 3010*

Taryn Saggese − *Te Papa Tipu Innovation Park, Rotorua, New Zealand 3010*

Maxime Barbier − *Te Papa Tipu Innovation Park, Rotorua, New Zealand 3010*

Miruna Petcu − *Te Papa Tipu Innovation Park, Rotorua, New Zealand 3010*

Mark West − *Te Papa Tipu Innovation Park, Rotorua, New Zealand 3010*

Beatrix Theobald − *Te Papa Tipu Innovation Park, Rotorua, New Zealand 3010*

Eva Gaugler − *Te Papa Tipu Innovation Park, Rotorua, New Zealand 3010*

Kate Parker − *Te Papa Tipu Innovation Park, Rotorua, New Zealand 3010*

Complete contact information is available at: https://pubs.acs.org/10.1021/acs.biomac.3c01077

https://doi.org/10.1021/acs.biomac.3c01077
Biomacromolecules 2024, 25, 455−465

Author Contributions

A.F.G. and R.A. contributed equally to the conceptualization of the idea, design of primary experiments, and authorship of this publication. A.A.V. contributed to the idea and design of key experiments. Y.C., Q.T., and B.T. performed experiments related to degradation of plastics and SEM and sensor fabrication. R.R. and M.B. contributed thermomechanical analysis of polymers, M.P. and E.G. contributed to the molecular weight analysis of degraded samples, and T.S. contributed to fluorescence microscopy experiments. K.P. and M.W. contributed to key evaluation of results.

Funding

This work was funded by the New Zealand Ministry of Business, Innovation and Employment (MBIE) in the framework of the Strategic Science Investment Fund.

Notes

The authors declare no competing financial interest.

■ ABBREVIATIONS

PBA, 1-pyrenebutyric acid; AL, Amano Lipase; CNF, carbon nanofiber; CNF_{PBA}, carbon nanofiber functionalized with PBA; CNF_{AL}, carbon nanofiber functionalized with Amano Lipase; PCL, polycaprolactone; CNF-PCL, composite made from PCL and CNF; CNF_{AL}-PCL, composite made from CNF_{AL} and PCL; CNF-AL_5-PCL, composite made from CNF, AL (5 wt %), and PCL; AL_1-PCL, composite made from AL (1 wt %) and PCL; AL_5-PCL, composite made from AL (5 wt %) and PCL.

■ REFERENCES

(1) Knott, B. C.; Erickson, E.; Allen, M. D.; Gado, J. E.; Graham, R.; Kearns, F. L.; Pardo, I.; Topuzlu, E.; Anderson, J. J.; Austin, H. P.; Dominick, G.; Johnson, C. W.; Rorrer, N. A.; Szostkiewicz, C. J.; Copié, V.; Payne, C. M.; Woodcock, H. L.; Donohoe, B. S.; Beckham, G. T.; McGeehan, J. E. Characterization and Engineering of a Two-Enzyme System for Plastics Depolymerization. *Proc. Natl. Acad. Sci. U. S. A.* **2020**, *117* (41), 25476−25485.

(2) Lu, H.; Diaz, D. J.; Czarnecki, N. J.; Zhu, C.; Kim, W.; Shroff, R.; Acosta, D. J.; Alexander, B. R.; Cole, H. O.; Zhang, Y.; Lynd, N. A.; Ellington, A. D.; Alper, H. S. Machine Learning-Aided Engineering of Hydrolases for PET Depolymerization. *Nature* **2022**, *604* (7907), 662−667.

(3) Son, H. F.; Cho, I. J.; Joo, S.; Seo, H.; Sagong, H.-Y.; Choi, S. Y.; Lee, S. Y.; Kim, K.-J. Rational Protein Engineering of Thermo-Stable PETase from Ideonella Sakaiensis for Highly Efficient PET Degradation. *ACS Catal.* **2019**, *9* (4), 3519−3526.

(4) Carrington, D., Ed.; D. C. E. New Super-Enzyme Eats Plastic Bottles Six Times Faster. *Guardian*, September 28, 2020. https://www.theguardian.com/environment/2020/sep/28/new-super-enzyme-eats-plastic-bottles-six-times-faster (accessed 2023-03-20).

(5) Can plastic-eating enzymes solve the recycling problem? https://channels.ft.com/en/rethink/can-plastic-eating-enzymes-solve-the-recycling-problem/ (accessed 2023-03-20).

(6) This AI-Designed Enzyme Can Devour Plastic Trash In Hours: Video. https://www.forbes.com/sites/davidrvetter/2022/04/28/scientists-use-ai-to-make-an-enzyme-that-eats-plastic-trash-in-hours-video/?sh=378e3466da6b (accessed 2023-03-20).

(7) An engineered PET depolymerase to break down and recycle plastic bottles|Nature. https://www.nature.com/articles/s41586-020-2149-4 (accessed 2023-03-20).

(8) Kortsha, M. *Plastic-eating Enzyme Could Eliminate Billions of Tons of Landfill Waste.* UT News . https://news.utexas.edu/2022/04/27/plastic-eating-enzyme-could-eliminate-billions-of-tons-of-landfill-waste/ (accessed 2023-03-20).

(9) Leitão, A. L.; Enguita, F. J. Structural Insights into Carboxylic Polyester-Degrading Enzymes and Their Functional Depolymerizing Neighbors. *Int. J. Mol. Sci.* **2021**, *22* (5), 2332.

(10) Rosato, A.; Romano, A.; Totaro, G.; Celli, A.; Fava, F.; Zanaroli, G.; Sisti, L. Enzymatic Degradation of the Most Common Aliphatic Bio-Polyesters and Evaluation of the Mechanisms Involved: An Extended Study. *Polymers* **2022**, *14* (9), 1850.

(11) Sayyed, R. Z.; Wani, S. J.; Alyousef, A. A.; Alqasim, A.; Syed, A.; El-Enshasy, H. A. Purification and Kinetics of the PHB Depolymerase of Microbacterium Paraoxydans RZS6 Isolated from a Dumping Yard. *PLoS One* **2019**, *14* (6), No. e0212324.

(12) Schwaminger, S. P.; Fehn, S.; Steegmüller, T.; Rauwolf, S.; Löwe, H.; Pflüger-Grau, K.; Berensmeier, S. Immobilization of PETase Enzymes on Magnetic Iron Oxide Nanoparticles for the Decomposition of Microplastic PET. *Nanoscale Adv.* **2021**, *3* (15), 4395−4399.

(13) Hegyesi, N.; Zhang, Y.; Kohári, A.; Polyák, P.; Sui, X.; Pukánszky, B. Enzymatic Degradation of PLA/Cellulose Nanocrystal Composites. *Ind. Crops Prod.* **2019**, *141*, No. 111799.

(14) Ganesh, M.; Dave, R. N.; L'Amoreaux, W.; Gross, R. A. Embedded Enzymatic Biomaterial Degradation. *Macromolecules* **2009**, *42* (18), 6836−6839.

(15) Greene, A. F.; Vaidya, A.; Collet, C.; Wade, K. R.; Patel, M.; Gaugler, M.; West, M.; Petcu, M.; Parker, K. 3D-Printed Enzyme-Embedded Plastics. *Biomacromolecules* **2021**, *22* (5), 1999−2009.

(16) DelRe, C.; Jiang, Y.; Kang, P.; Kwon, J.; Hall, A.; Jayapurna, I.; Ruan, Z.; Ma, L.; Zolkin, K.; Li, T.; Scown, C. D.; Ritchie, R. O.; Russell, T. P.; Xu, T. Near-Complete Depolymerization of Polyesters with Nano-Dispersed Enzymes. *Nature* **2021**, *592* (7855), 558−563.

(17) Huang, Q.; Hiyama, M.; Kabe, T.; Kimura, S.; Iwata, T. Enzymatic Self-Biodegradation of Poly(l-Lactic Acid) Films by Embedded Heat-Treated and Immobilized Proteinase K. *Biomacromolecules* **2020**, *21* (8), 3301−3307.

(18) Thoden van Velzen, E. U.; Santomasi, G. Tailor-Made Enzymes Poised to Propel Plastic Recycling into a New Era. *Nature* **2022**, *604* (7907), 631−633.

(19) New process makes 'biodegradable' plastics truly compostable| College of Chemistry. https://chemistry.berkeley.edu/news/new-process-makes-%E2%80%98biodegradable%E2%80%99-plastics-truly-compostable-0 (accessed 2023-03-21).

(20) Compostables-Packaging-Position-Statement.Pdf. https://environment.govt.nz/assets/publications/compostables-packaging-position-statement.pdf (accessed 2023-03-21).

(21) Suciu, G.; Ciuciuc, R.; Pasat, A.; Scheianu, A. Remote Sensing for Forest Environment Preservation. In *Recent Advances in Information Systems and Technologies*; Rocha, Á., Correia, A. M., Adeli, H., Reis, L. P., Costanzo, S., Eds.; Springer International Publishing: Cham, 2017; pp 211−220 Advances in Intelligent Systems and Computing.

(22) Torresan, C.; Benito Garzón, M.; O'Grady, M.; Robson, T. M.; Picchi, G.; Panzacchi, P.; Tomelleri, E.; Smith, M.; Marshall, J.; Wingate, L.; Tognetti, R.; Rustad, L. E.; Kneeshaw, D. A New Generation of Sensors and Monitoring Tools to Support Climate-Smart Forestry Practices. *Can. J. For. Res.* **2021**, *51* (12), 1751−1765.

(23) Wiesemüller, F.; Miriyev, A.; Kovac, M. Zero-Footprint Eco-Robotics: A New Perspective on Biodegradable Robots. *2021 Aerial Robotic Systems Physically Interacting with the Environment (AIRPHARO)* **2021**, 1−6.

(24) Li, W.; Liu, Q.; Zhang, Y.; Li, C.; He, Z.; Choy, W. C. H.; Low, P. J.; Sonar, P.; Kyaw, A. K. K. Biodegradable Materials and Green Processing for Green Electronics. *Adv. Mater.* **2020**, *32* (33), No. 2001591.

(25) Zhu, H.; Luo, W.; Ciesielski, P. N.; Fang, Z.; Zhu, J. Y.; Henriksson, G.; Himmel, M. E.; Hu, L. Wood-Derived Materials for Green Electronics, Biological Devices, and Energy Applications. *Chem. Rev.* **2016**, *116* (16), 9305−9374.

(26) Piro, B.; Tran, H. V.; Thu, V. T. Sensors Made of Natural Renewable Materials: Efficiency, Recyclability or Biodegradability—The Green Electronics. *Sensors* **2020**, *20* (20), 5898.

(27) Abbel, R.; Greene, A. F.; Quilter, H.; Leveneur, J.; Risani, R.; Barbier, M.; West, M.; Collet, C.; Kirby, N. M.; Sorieul, M. Crystallization Behavior and Sensing Properties of Bio-Based Conductive Composite Materials. *Adv. Eng. Mater.* **2023**, *25* (2), No. 2200959.
(28) Beniwal, A.; Ganguly, P.; Aliyana, A. K.; Khandelwal, G.; Dahiya, R. Screen-Printed Graphene-Carbon Ink Based Disposable Humidity Sensor with Wireless Communication. *Sens. Actuators B Chem.* **2023**, *374*, No. 132731.
(29) Tu, T.; Liang, B.; Cao, Q.; Fang, L.; Zhu, Q.; Cai, Y.; Ye, X. Fully Transient Electrochemical Testing Strips for Eco-Friendly Point of Care Testing. *RSC Adv.* **2020**, *10* (12), 7241−7250.
(30) Challenges and opportunities of biodegradable plastics: A mini review - Maja Rujnić-Sokele, Ana Pilipović, 2017. https://journals.sagepub.com/doi/abs/10.1177/0734242X16683272?journalCode=wmra (accessed 2023-03-21).
(31) Iwata, T. Biodegradable and Bio-Based Polymers: Future Prospects of Eco-Friendly Plastics. *Angew. Chem., Int. Ed.* **2015**, *54* (11), 3210−3215.
(32) Kwon, J.; DelRe, C.; Kang, P.; Hall, A.; Arnold, D.; Jayapurna, I.; Ma, L.; Michalek, M.; Ritchie, R. O.; Xu, T. Conductive Ink with Circular Life Cycle for Printed Electronics. *Adv. Mater.* **2022**, *34* (30), No. 2202177.
(33) Bozó, É.; Ervasti, H.; Halonen, N.; Shokouh, S. H. H.; Tolvanen, J.; Pitkänen, O.; Järvinen, T.; Pálvölgyi, P. S.; Szamosvölgyi, Á.; Sápi, A.; Konya, Z.; Zaccone, M.; Montalbano, L.; De Brauwer, L.; Nair, R.; Martínez-Nogués, V.; San Vicente Laurent, L.; Dietrich, T.; Fernández de Castro, L.; Kordas, K. Bioplastics and Carbon-Based Sustainable Materials, Components, and Devices: Toward Green Electronics. *ACS Appl. Mater. Interfaces* **2021**, *13* (41), 49301−49312.
(34) Phosphate Buffer (pH 5.8 to 7.4) Preparation and RecipelAAT Bioquest. https://www.aatbio.com/resources/buffer-preparations-and-recipes/phosphate-buffer-ph-5-8-to-7-4 (accessed 2023-03-21).
(35) Min, K.; Kim, J.; Park, K.; Yoo, Y. J. Enzyme Immobilization on Carbon Nanomaterials: Loading Density Investigation and Zeta Potential Analysis. *J. Mol. Catal. B Enzym.* **2012**, *83*, 87−93.
(36) Chang, S. K. C.; Zhang, Y. Protein Analysis. In *Food Analysis*; Nielsen, S. S., Ed.; Springer International Publishing: Cham, 2017; pp 315−331. Food Science Text Series.
(37) Baptista, C.; Azagury, A.; Shin, H.; Baker, C. M.; Ly, E.; Lee, R.; Mathiowitz, E. The Effect of Temperature and Pressure on Polycaprolactone Morphology. *Polymer* **2020**, *191*, No. 122227.
(38) Skoglund, P.; Fransson, Å. Continuous Cooling and Isothermal Crystallization of Polycaprolactone. *J. Appl. Polym. Sci.* **1996**, *61* (13), 2455−2465.

https://doi.org/10.1021/acs.biomac.3c01077
Biomacromolecules 2024, 25, 455−465